

EASR**Engineering and Applied Science Research**<https://www.tci-thaijo.org/index.php/easr/index>

Published by the Faculty of Engineering, Khon Kaen University, Thailand

Modelling approach to nitrate adsorption on triamine-bearing activated rice husk ashPhuoc Toan Phan^{1, 2, 3)}, Thai Anh Nguyen⁴⁾, Nhat Huy Nguyen^{1, 2)} and Trung Thanh Nguyen^{*2, 5)}¹⁾Faculty of Environment and Natural Resources, Ho Chi Minh City University of Technology, Ho Chi Minh City, Vietnam²⁾Vietnam National University, Ho Chi Minh City, Vietnam³⁾Faculty of Engineering, Technology, Environment, An Giang University, An Giang Province, Vietnam⁴⁾Faculty of Chemical and Food Technology, Ho Chi Minh City University of Technology and Education, Ho Chi Minh City, Vietnam⁵⁾Nanomaterial Laboratory, An Giang University, An Giang Province, Vietnam

Received 16 August 2019

Revised 11 November 2019

Accepted 16 December 2019

Abstract

This work presents a systematic study of nitrate removal using amine grafted activated rice husk ash by batch adsorption. The effects of solution pH, adsorption time, amount of adsorbent, adsorption temperature, and initial nitrate concentration were investigated. Various adsorption models, such as Langmuir, Freundlich, Tempkin, Redlich-Peterson, and Dubinin-Radushkevich, were applied to determine the adsorption nature of this system. The most suitable model was found to be the Redlich-Peterson model for describing this adsorption process. Moreover, the adsorption process was endothermic and spontaneous, as shown by the obtained thermodynamic parameters. Finally, the competitive effect of inorganic anions was also evaluated and their effect was found to be in the descending order of $\text{PO}_4^{3-} > \text{SO}_4^{2-} > \text{HCO}_3^- > \text{Cl}^-$.

Keywords: Nitrate adsorption, Rice husk ash, Water treatment**1. Introduction**

Nitrate pollution of water sources is becoming a serious problem globally due to the use of nitrogenous fertilizer in agriculture and discharge of untreated nitrogen-rich wastewater effluents [1]. In the human body, nitrate ions can be reduced to nitrite in combination with hemoglobin to form methaemoglobin, which adversely affects human health and causes death at high levels [2-3]. The highest allowable concentration of nitrates in drinking water recommended by the World Health Organization is $50 \text{ mgNO}_3^-/\text{L}$ ($\sim 11.3 \text{ mgNO}_3^-/\text{N/L}$).

Current techniques of removing nitrate still have certain limitations. For example, bio-denitrification processes need strictly controlled operating condition in terms of pH, temperature, and additional organic matter [4]. Reverse osmosis and membrane filtration techniques are costly [5]. Heterogeneous catalytic processes can produce secondary pollution while ion exchange resins are often unstable at high temperature and inefficient at low temperature [6]. Recently, nitrate adsorption using materials derived from agricultural by-products have attracted much attention. This is due to simplicity, high efficiency, low cost, and environmental-friendly components, which simultaneously solve many pollution issues [7-9]. Orlando *et al.* [10] incorporated epoxy/amines into bagasse, rice husks, and pure cellulose and applied them for nitrate removal. Maximal nitrate

adsorption capacity of $\sim 87.42 \text{ mg/g}$ and $\sim 81.84 \text{ mg/g}$ was achieved using bagasse and rice husks, respectively. This is comparable to using pure cellulose, $\sim 83.08 \text{ mg/g}$. Wheat straw modified with epichlorohydrin and dimethylamine was used for nitrate removal with maximal nitrate adsorption of 128.96 mg/g [11]. Additionally, other materials such as corn stalks, sugar beet pulp, and modified wheat residues were utilized and modified for nitrate adsorption [12-14]. The amount of available waste rice husks is high countries such as Vietnam. Currently rice husks are used as fuel in various industrial processes such as providing heat for brick kilns or drying agricultural products. As a result, large amount of rice husk ash (RHA) generated and an effective solution for reuse of this waste has not yet been found. Therefore, use of rice husk ash for nitrate removal from water is quite attractive. In a recent publication [15], we reported successful synthesis of triamine grafted activated RHA with a higher nitrate adsorption capacity (163.4 mg/g) than a commercial anion exchange resin (Aqualite A420). However, that work only focused on material synthesis and characterization. The nature and mechanism of nitrate adsorption on the material surface was not systematically studied.

The current study is a detailed investigation of the effect of experimental conditions such as pH, adsorption time, amount of adsorbent, nitrate concentration, and temperature on adsorption capacity. The adsorption kinetics, isothermal behavior, and thermodynamics were studied to explore the

*Corresponding author. Tel.: +849 4324 0380

Email address: ntthanh@agu.edu.vn

doi: 10.14456/easr.2020.21

nature of the adsorption process. Anion competition testing was conducted to determine the effect of common anions in actual water environment on the adsorption of nitrate.

2. Materials and methodology

2.1 Preparation and characterization of adsorbent materials

In this study, the adsorbent material used was triamine-bearing activated rice husk ash (TRI-ARHA) synthesized from rice husk ash generated from brick kilns in An Giang Province, Vietnam [15]. Characteristics of chemical composition on the surface of TRI-ARHA before and after nitrate ion adsorption was determined using Fourier Transform Infrared Spectrometry (FTIR) (Alpha-Bruker, Germany) over the spectrum from 500 to 4000 cm^{-1} .

2.2 Nitrate adsorption isotherms

The adsorption capability of the synthesized materials was evaluated using a batch nitrate adsorption test. A mass of adsorbent, 0.005 - 0.100 g, was mixed with 50 mL of an aqueous nitrate solution (pH 3 – 10, nitrate concentration of 50 – 600 $\text{mgNO}_3\text{-N/L}$) and the mixture was shaken at 120 rpm and 15 – 45 °C in a thermostatic water-bath shaker. After 1 – 20 min, the adsorbent was separated by centrifugation at 10,000 rpm and nitrate concentration of the supernatant was determined using UV-visible spectrophotometry (SPECORD 210 Plus, Analytik Jena, Germany) with a sodium salicylate reagent at a wavelength of 410 nm. All experiments were replicated three times and the nitrate adsorption capacity was calculated using Equation 1.

Adsorption isotherms are preferred for their ease of modeling experimental adsorption data. Langmuir and Freundlich models are generally used because they are simple and applicable over a wide range of concentrations. Homogeneous adsorption is assumed according to Langmuir theory, or a single molecular layer is formed when adsorption takes place with no other adsorption in that position [12]. For adsorption processes that occur on heterogenous surfaces or for multi-layer adsorption, the Freundlich isotherm is more applicable since its expression defines exponential distribution of active sites, their energies and the nature of surface heterogeneity [16]. For the Redlich-Peterson isotherm, the main factors contributing to the Langmuir and Freundlich models are combined to form this empirical isotherm. Therefore, the ideal monolayer adsorption theory does not completely dominate this model. Alternatively, adsorbent–adsorbate interactions are assumed in the Temkin isotherm model. Heat of sorption decreases linearly with these interactions. Then the binding energy is uniformly distributed and increases to a maximum value. Contrary to the implications of the Freundlich equation that the relationship of reduced-adsorption heat is logarithmic, the linear form assumes a derivation of the Temkin isotherm. Finally, for adsorption mechanisms with Gaussian energy distributions onto heterogeneous surfaces [17], the Dubinin-Radushkevich isotherm model is usually applied to distinguish physical and chemical adsorption based on mean adsorption energy E [16].

The nonlinear forms of Langmuir, Freundlich, Temkin, Redlich-Peterson, and Dubinin-Radushkevich isotherms are represented in Equation 2, 3, 4, 5, and 6, respectively. The mean free energy, E , of the Dubinin-Radushkevich model can be expressed as Equation 7 [17].

$$Q_e = \frac{C_0 - C_e}{m} \times V \quad (1)$$

$$Q_e = \frac{K_L Q_{max} C_e}{1 + K_L C_e} \quad (2)$$

$$Q_e = K_F C_e^{1/n} \quad (3)$$

$$Q_e = \frac{RT}{b_T} \ln(a_T C_e) \quad (4)$$

$$Q_e = \frac{\alpha C_e}{1 + K_{RP} C_e^n} \quad (5)$$

$$Q_e = Q_{max} \exp\left(-\beta \left(RT \ln\left(1 + \frac{1}{C_e}\right)\right)^2\right) \quad (6)$$

$$E = \frac{1}{\sqrt{2\beta}} \quad (7)$$

where C_0 and C_e (mg/L) are nitrate concentrations at initial and equilibrium states, respectively. V (50 mL) and m (mg) are the volume of the experimental solution and adsorbent amount, respectively. Q_e (mg/g) is the quantity of nitrate ions adsorbed and Q_{max} (mg/g) is the maximum adsorption capacity. K_L (L/mg) is the Langmuir constant obtained at equilibrium time and is closely related to adsorption energy. K_F (L/mg) and n are Freundlich constants. b_T (J/mol) and a_T are Temkin constants while R (8.314 J/mol.K) and T (K) are the ideal gas constant and absolute temperature, respectively. α (L/g) and K_{RP} (L/mg) are Redlich-Peterson constants while β (mol^2/kJ^2) and E (kJ/mol) are the Dubinin-Radushkevich constant and mean adsorption energy, respectively.

In parallel with the calculation of adsorption parameters using the above equations, it is necessary to determine their deviations to evaluate the compatibility of these models. The smaller the value of χ^2 , the less the difference between the Q_{max} value obtained from the model and the experiment data, or in other words, the model's compatibility with experimental data increases. The chi-square model has been applied in this case as the mathematical function expressed as follows: [12]

$$\chi^2 = \sum \frac{(Q_{max,exp} - Q_{max,cal})^2}{Q_{max,cal}} \quad (8)$$

where $Q_{max,cal}$ (mg/g) and $Q_{max,exp}$ (mg/g) are the maximum adsorption capacity obtained from the linear regression of the isotherm model and the experiment data.

2.3 Adsorption thermodynamics

Adsorption thermodynamics were studied by performing the adsorptions at various temperatures. The values of ΔG (Gibbs free energy), ΔH° (change in enthalpy), and ΔS° (change in entropy) were calculated as follows [18]:

$$\Delta G = -RT \ln K \quad (9)$$

$$\ln K = \frac{\Delta S}{R} - \frac{\Delta H}{RT} \quad (10)$$

where ΔG (kJ/mol) and T (K) are the free energy change and absolute temperature, respectively. $R = 8.314$ J/mol.K and $K = K_L$ from Equation 2.

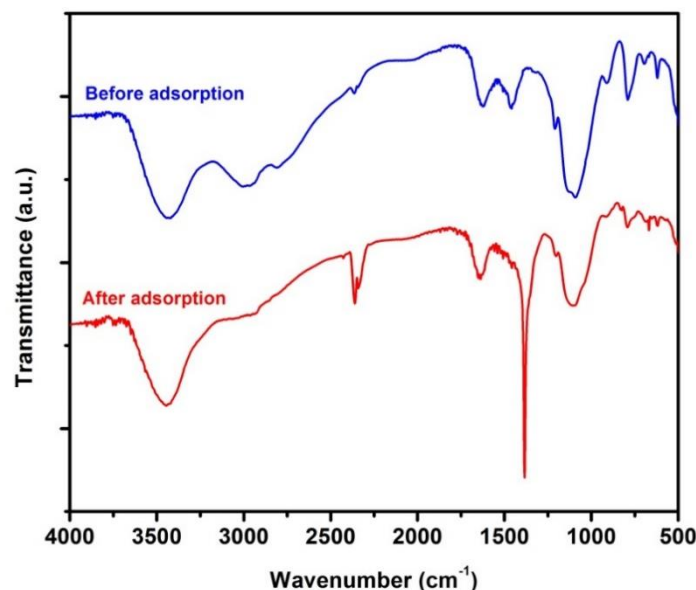


Figure 1 FTIR results of fresh and nitrate adsorbed TRI-ARHA

2.4 Adsorption kinetics

A kinetics study was conducted with four models (pseudo-first-order, modified-pseudo-first-order, pseudo-second-order and intra-particle diffusion, expressed as Equation 11 – 14, respectively). Then, they were employed for describing the experimental kinetic data [12].

$$\ln(Q_e - Q_t) = \ln Q_e - k_1 t \quad (11)$$

$$\frac{Q_t}{Q_e} + \ln(Q_e - Q_t) = \ln Q_e - K_1 t \quad (12)$$

$$\frac{t}{Q_t} = \frac{1}{k_2 Q_e^2} + \frac{t}{Q_e} \quad (13)$$

$$Q_t = k_{ip} t^{0.5} \quad (14)$$

where Q_e and Q_t (both in mg/g) are adsorption capacity of TRI-ARHA at the time of equilibrium and at time t (min), respectively. k_1 (1/min), K_1 (1/min), k_2 (g/mg.min), and k_{ip} (mg/g.min) are the rate constants of their corresponding models.

3. Results and discussion

3.1 FTIR results of adsorbent material

The FTIR spectra in Figure 1 demonstrate the specific change in the structure of the TRI-ARHA as a result of nitrate ion adsorption on TRI-ARHA surfaces. The -NH_2 and -OH groups stretching vibrations are identified by the presence of a peak at 3424 cm^{-1} . Typical fluctuations of silica composition in RHA structure are confirmed by Si-O-Si and Si-H bonds, which are indicated by the peaks at 1091 and $620\text{-}912 \text{ cm}^{-1}$, respectively [19]. The peak at 1382 cm^{-1} represents N-O stretching [20] and its sharp appearance displays the effectiveness of nitrate ion adsorption. Stretching vibrations of C=O, C-N, and C-O were observed with peaks at 1625 , 1458 , and 1118 cm^{-1} , respectively, which

show the presence of a protonated form of triamine groups [21]. The C-N peak (1458 cm^{-1}) strongly shifted toward the peak of N-O stretching (1382 cm^{-1}) after adsorption. This evidence reveals the efficiency of nitrate adsorption carried out through the ion exchange mechanism at the amine groups [12].

3.2 Effect of initial solution pH and material dosage on nitrate adsorption

Preliminary investigation of the effects of pH and adsorbent dosage were first performed since they are usually factors that greatly affect the ion adsorption capacity. The adsorption tests were run at solution pH values in the range of 3 – 10 and a nitrate concentration of 50 mg/L . As presented in Figure 2, nitrate adsorption capacity of TRI-ARHA was higher than 16 mg/g in pH range from 3 to 8. At pH 7, it reached the highest capacity of 31.35 mg/g and then decreased rapidly with the further increase of pH from 7 to 10. This may be due to the effect of solution pH on both the adsorbent surface and nitrate speciation [22]. It is generally true that an increase in pH results in the surfaces becoming negatively charged, which create an unfavorable condition for nitrate adsorption due to electrostatic repulsion [20]. In an acidic environment (e.g. $\text{pH} < 5$), nitrate ions may have been protonated and the electrostatic interaction between these nitrate ions and the adsorption centers on the TRI-ARHA surface are weakened. In an alkaline environment ($\text{pH} > 8$), an adsorption competition between OH^- ions with nitrate ions appears.

Figure 3 shows the significant effect of TRI-ARHA dosage on nitrate adsorption. The degree of nitrate ion uptake in TRI-ARHA reached its highest value of 71.83 mg/g at the lowest adsorbent amount of 0.1 g/L , but decreased to 24.62 mg/g at the highest amount of 2.0 g/L . This showed that the TRI-ARHA material can be applied for nitrate removal. The amount of TRI-ARHA needed for the efficient nitrate adsorption is 0.6 mg/L in terms of both treatment efficiency and adsorption capacity.

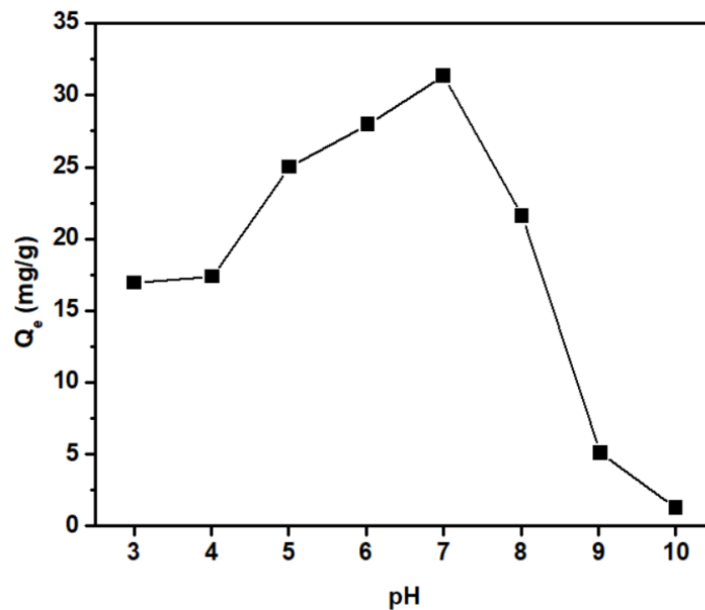


Figure 2 Nitrate removal with various initial solution pH values
(Conditions: temperature: 25 ± 0.5 °C, dosage: 0.6 g/L, nitrate: 50 mg/L, time: 10 min)

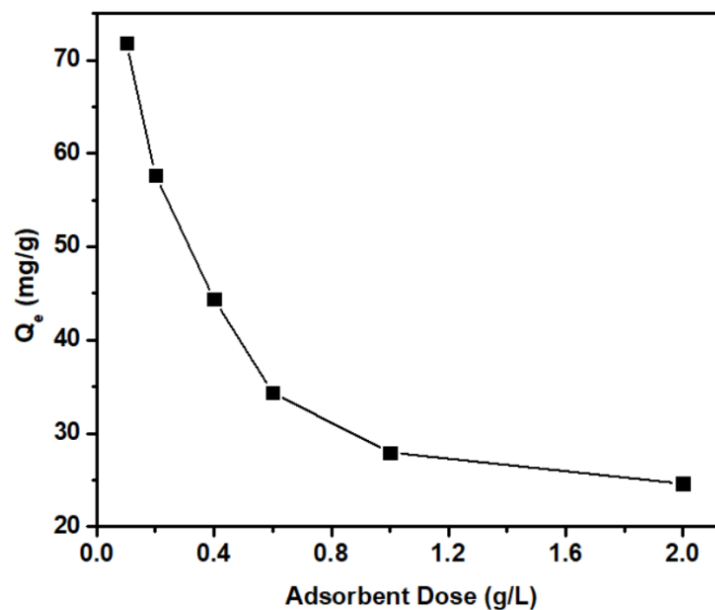


Figure 3 Nitrate removal using various amounts of adsorbent
(Conditions: temperature: 25 ± 0.5 °C, pH 7, nitrate: 50 mg/L, time: 10 min)

3.3 Adsorption isotherms

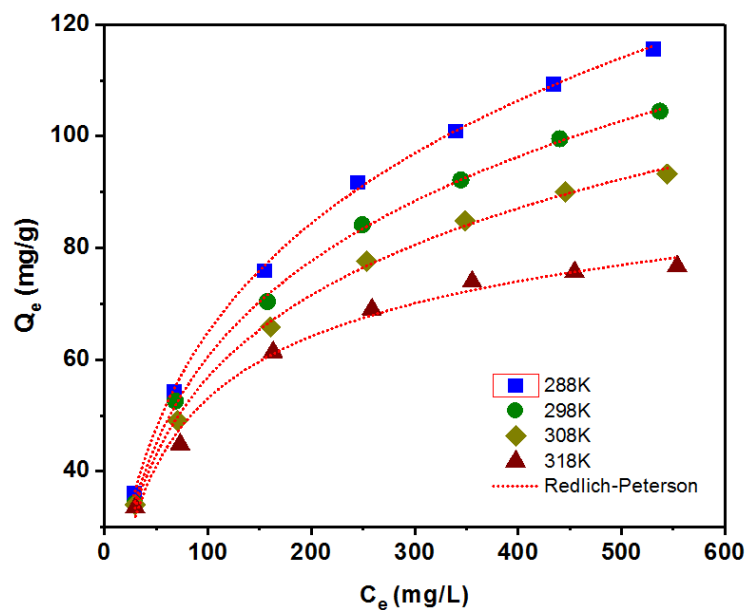
The effectiveness of adsorption modelling is generally confirmed by evaluating its correlation coefficient (r^2). The Redlich-Peterson model has been shown the most suitable owing to its highest r^2 value (0.9991) and lowest χ^2 (0.7353) (Table 1 and Figure 4). These results are in agreement with a previous study in which the Redlich-Peterson equation was used to improve the fitting of the Langmuir or Freundlich equations [23]. The empirical Freundlich equation is commonly applied for multilayer adsorption on an adsorbent with heterogeneous surfaces [24-25]. Adsorption is more favorable when n is larger than 1. Table 1 shows that the n value (~ 2.66) is much larger than 1 and the Freundlich model has a much lower χ^2 value than the Langmuir model. Thus,

the Freundlich model is considered a better fitting model than the Langmuir equation. Additionally, the mechanism of adsorption of nitrate ions on TRI-ARHA material is more likely to be a multilayer type. Moreover, the q_{\max} values in this study are 4.0-fold ($\sim 117.4/29.2$) to 12.6-fold ($\sim 117.4/9.3$) higher than previously reported for various activated carbons [26]. Additionally, the Temkin model accounts for the reduction in heat of adsorption according to a linear trend. Its adsorption nature is also evaluated based on the Freundlich (K_F) and Temkin constants (b_T) [27]. These constants both increase with temperature, suggesting that the process of nitrate adsorption on this adsorbent is endothermic [20].

In Dubinin-Radushkevich isotherms, the nature of adsorption can be determined using the calculated mean

Table 1 Adsorption parameters of isotherm models at various temperatures

Isotherm model	Adsorption parameters	Adsorption temperature (K)			
		288	298	308	318
Langmuir	Q_{\max} (mg/g)	132.40	117.39	103.64	84.062
	K_L (L/mg)	0.0102	0.0114	0.0131	0.0182
	R^2	0.9784	0.9780	0.9771	0.9790
	χ^2	18.797	14.692	11.340	5.9591
Freundlich	K_F ((mg/g)(L/mg) ⁿ)	11.219	11.417	12.087	14.429
	n	2.6632	2.8093	3.0344	3.6658
	R^2	0.9926	0.9904	0.9877	0.9595
	χ^2	6.4439	6.4157	6.0871	11.510
Tempkin	a_T (L/g)	0.1163	0.1294	0.1584	0.2732
	b_T (J/mol)	86.929	101.84	122.24	167.49
	R^2	0.9919	0.9955	0.9960	0.9853
	χ^2	7.0699	3.0002	1.9901	4.1671
Redlich-Peterson	a (L/g)	3.1510	2.8935	2.8450	2.2329
	K_{RP} (L/mg)	0.1241	0.1084	0.1028	0.0526
	n	0.7462	0.7713	0.7954	0.8930
	R^2	0.9991	0.9989	0.9977	0.9854
Dubinin-Radushkevich	χ^2	0.7734	0.7353	1.1321	4.1578
	Q_{\max} (mg/g)	98.441	89.846	81.478	70.099
	β (mol ² /kJ ²)	$2.258 \cdot 10^{-4}$	$2.009 \cdot 10^{-4}$	$1.640 \cdot 10^{-4}$	$1.229 \cdot 10^{-4}$
	E (kJ/mol)	47.056	49.893	55.223	63.784
	R^2	0.6757	0.7021	0.6907	0.7162

**Figure 4** Isotherm curves of the Redlich-Peterson model (Conditions: dosage: 0.6 g/L, pH 7, contact time: 10 min)

adsorption energy E . Generally, the process is more likely to be chemical in nature with E values higher than 8-16 kJ/mol. Otherwise, it involves physical adsorption [17, 28]. The calculated experimental value of E from in this study was in range of 47.1-63.8 kJ/mol (Table 1), possibly due to chemical adsorption of nitrate ions on the surface of TRI-ARHA.

3.4 Adsorption thermodynamics

Table 2 gives free energy, enthalpy, and entropy changes during the adsorption of nitrate on TRI-ARHA. An endothermic process is reflected in the positive value of ΔH . However, Table 1 shows that decreasing temperature simultaneously results in more nitrate adsorbed. This

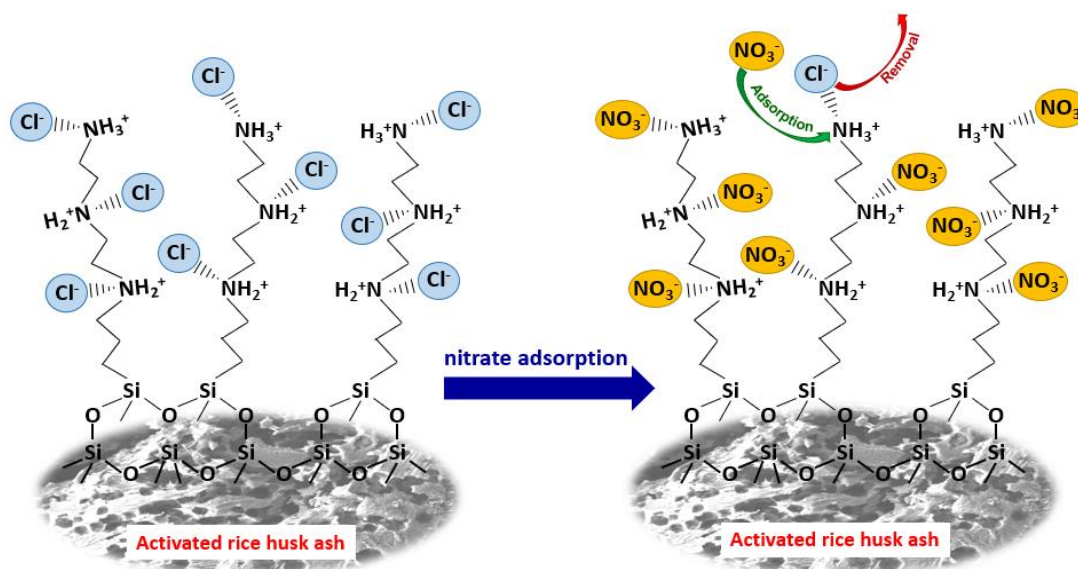
phenomenon occurs because of nitrate adsorption interference caused by Cl^- ions released after adsorption of nitrate ions (Figure 5). The positive value of ΔS suggests that the system exhibits random behavior [28], and this trend of entropy change suggests an increase in the randomness of Cl^- ions at the adsorbent surface during adsorption. The strong movement of Cl^- ions with increased temperature hinders the absorption of nitrate ions onto TRI-ARHA adsorbent. Therefore, a lower equilibrium nitrate adsorption was observed with higher temperature, physically involving weak forces of attraction. Additionally, the adsorption nature is spontaneous and feasible when ΔG has a negative value [22]. The standard free energy was in range of 11.88 to 14.65 kJ/mol (between 8 and 16 kJ/mol), thus ion exchange is considered to be the major contributor to adsorption

Table 2 Thermodynamic parameters of nitrate adsorption on TRI-ARHA at various temperatures (nitrate concentration: 50 mg/L)

ΔH (kJ/mol)	ΔS (kJ/mol.K)	ΔG (kJ/mol)				R^2
		288 K	298 K	308 K	318 K	
14.2	0.09	-11.88	-12.56	-13.34	-14.65	0.9146

Table 3 Kinetic parameters for adsorption of nitrate ions on TRI-ARHA

Model	Parameters	Initial Concentration		
		50 ppm	100 ppm	200 ppm
Pseudo-first-order	$Q_{e,cal}$ (mg/g)	17.972	27.037	22.160
	k_1 (min^{-1})	0.0646	0.1633	0.2409
	R^2	0.4825	0.6173	0.7802
Modified-pseudo-first-order	$Q_{e,cal}$ (mg/g)	27.707	41.030	42.798
	K_1 (min^{-1})	0.0396	0.1275	0.2182
	R^2	0.4731	0.6134	0.8036
Pseudo-second-order	$Q_{e,cal}$ (mg/g)	32.362	65.789	76.336
	k_2 ($\text{g}\cdot\text{mg}^{-1}\cdot\text{min}^{-1}$)	0.0133	0.0034	0.0107
	R^2	0.9698	0.9295	0.9915
Intra-particle diffusion	k_{ip} ($\text{mg}\cdot\text{g}^{-1}\cdot\text{min}^{-1/2}$)	5.6224	11.933	10.560
	I	7.7275	6.6782	32.577
	R^2	0.6263	0.7034	0.5632

**Figure 5** Nitrate adsorption mechanism of TRI-ARHA

[17, 29]. Furthermore, the more positive values of ΔG with increasing temperature indicates that the adsorption process tends to proceed more rapidly at low temperatures [30].

3.5 Adsorption kinetics

Figure 6 shows the change in the amount of nitrate adsorbed on TRI-ARHA over time. A linear regression result of the pseudo-second-order (PSO) equation (Table 3) has a correlation coefficient (R^2) that is greater than 0.92, and value of the calculated adsorption capacity ($Q_{e,cal}$) reached 76.34 mg/g corresponding to 200 ppm of the initial nitrate concentration. The values of these parameters for the PSO model are higher than for other models. Hence, in this work, the best-fitting equation for this nitrate removal is the PSO model. Moreover, this fit suggests that adsorption takes place at the surface of the adsorbent, or that the adsorption process involves an ion exchange mechanism.[12, 30]

3.6 Effect of other anions

In addition to nitrate, other anions such as Cl^- , HCO_3^- , SO_4^{2-} , and PO_4^{3-} are often present in natural water sources and wastewater effluents. These anions tend to interact with adsorbent surfaces and reduce nitrate removal. Hence, the competitive effect of inorganic anions such as PO_4^{3-} , SO_4^{2-} , HCO_3^- , and Cl^- on the nitrate adsorption on TRI-ARHA was considered. The results in Figure 7 show that co-existing inorganic anions have an effect that reduces nitrate adsorption by TRI-ARHA materials. The degree of reduction is proportional to the concentration of competitive ions. This may be due to the hydration energies of Cl^- , HCO_3^- , SO_4^{2-} , and PO_4^{3-} ions and the electrostatic interactions with adsorption centers of TRI-ARHA materials are much stronger than that of NO_3^- ions [12]. In summary, the degree of the negative effects of inorganic anions can be arranged in a descending order as $\text{PO}_4^{3-} > \text{SO}_4^{2-} > \text{HCO}_3^- > \text{Cl}^-$ [12].

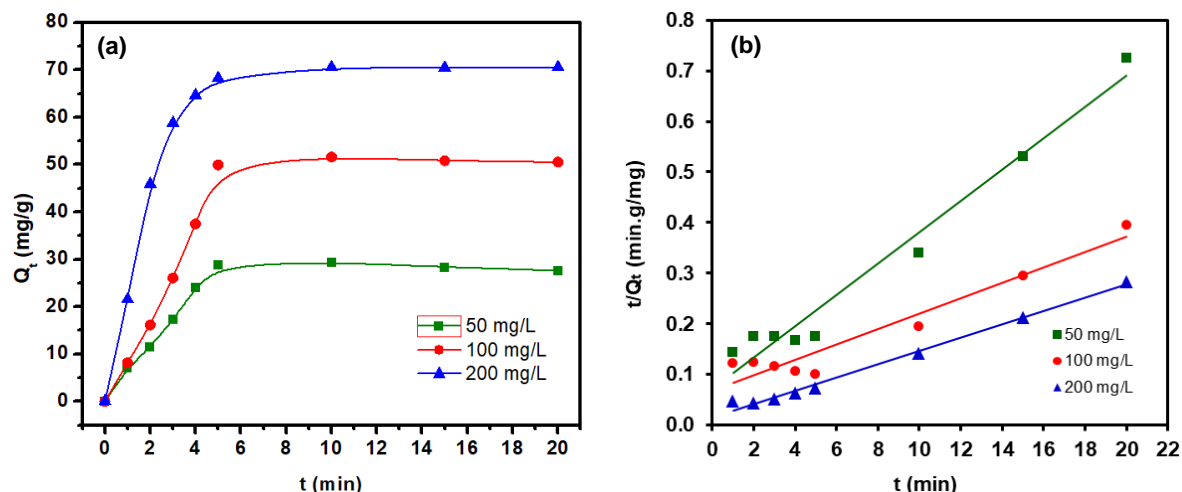


Figure 6 (a) Time changes of the amount of nitrate adsorbed and (b) the linear plot of pseudo-second-order model for nitrate adsorption (Conditions: dosage: 0.6 g/L, pH 7, temperature: 25 ± 0.5 °C)

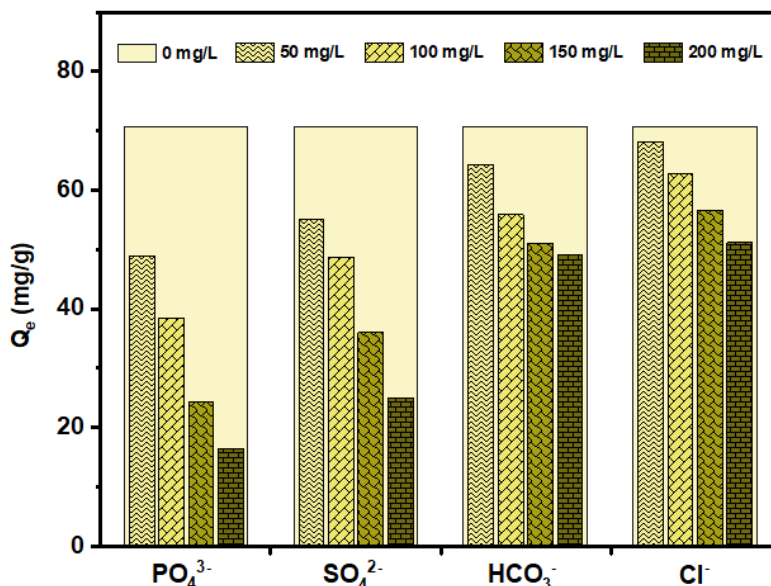


Figure 7 Uptake of nitrate by TRI-ARHA with other anions in solution (Conditions: dosage: 0.6 g/L, pH 7, temperature: 25 ± 0.5 °C, contact time: 10 min)

4. Conclusions

TRI-ARHA has many outstanding advantages, including high nitrate adsorption capacity, short time required for nitrate removal, and a wide range of effective pH values. The experimental adsorption data were best fit by the Redlich-Peterson isotherm and pseudo-second-order kinetics models. The obtained parameters from our thermodynamic study revealed that the adsorption of nitrate on TRI-ARHA is an endothermic and spontaneous process by chemical adsorption. The negative effects of inorganic anions on the adsorption of nitrate on this material were in a descending order of $PO_4^{3-} > SO_4^{2-} > HCO_3^- > Cl^-$.

5. Acknowledgements

This research is funded by Vietnam National University - Ho Chi Minh City under grant number A2020-16-01.

6. References

- [1] Ghafari S, Hasan M, Aroua MK. Bio-electrochemical removal of nitrate from water and wastewater-a review. *Bioresour Technol.* 2008;99(10):3965-74.
- [2] Majumdar D, Gupta N. Nitrate pollution of groundwater and associated human health disorders. *Indian J Environ Hlth.* 2000;42(1):28-39.
- [3] WHO. *Guidelines for Drinking-Water Quality.* Geneva: World Health Organization; 1993.
- [4] Park JJ, Byun IG, Park SR, Lee JH, Park SH, Park TJ, et al. Use of spent sulfidic caustic for autotrophic denitrification in the biological nitrogen removal processes: Lab-scale and pilot-scale experiments. *J Ind Eng Chem.* 2009;15(3):316-22.
- [5] Malaeb L, Ayoub GM. Reverse osmosis technology for water treatment: State of the art review. *Desalination.* 2011;267(1):1-8.

- [6] Bhatnagar A, Sillanpää M. A review of emerging adsorbents for nitrate removal from water. *Chem Eng J.* 2011;168(2):493-504.
- [7] Ahmaruzzaman M, Gupta VK. Rice Husk and its ash as low-cost adsorbents in water and wastewater treatment. *Ind Eng Chem Res.* 2011;50(24):13589-613.
- [8] Tyagi S, Rawtani D, Khatri N, Tharmavaram M. Strategies for nitrate removal from aqueous environment using nanotechnology: a review. *J Water Process Eng.* 2018;21:84-95.
- [9] Joseph F, Agrawal YK, Rawtani D. Behavior of malachite green with different adsorption matrices. *Front Life Sci.* 2013;7(3-4):99-111.
- [10] Orlando US, Baes AU, Nishijima W, Okada M. A new procedure to produce lignocellulosic anion exchangers from agricultural waste materials. *Bioresour Technol.* 2002;83(3):195-8.
- [11] Wang Y, Gao B-y, Yue W-w, Yue Q-y. Preparation and utilization of wheat straw anionic sorbent for the removal of nitrate from aqueous solution. *J Environ Sci.* 2007;19(11):1305-10.
- [12] Song W, Gao B, Xu X, Wang F, Xue N, Sun S, et al. Adsorption of nitrate from aqueous solution by magnetic amine-crosslinked biopolymer based corn stalk and its chemical regeneration property. *J Hazard Mater.* 2016;304:280-90.
- [13] Hassan M, Kassem N, H. Abd El-Kader A. Novel Zr(IV)/sugar beet pulp composite for removal of sulfate and nitrate anions. *J Appl Polym Sci.* 2010;117(4):2205-12.
- [14] Wang Y, Gao BY, Yue WW, Yue QY. Adsorption kinetics of nitrate from aqueous solutions onto modified wheat residue. *Colloids Surf A Physicochem Eng Asp.* 2007;308(1):1-5.
- [15] Phan PT, Nguyen TT, Nguyen NH, Padungthon S. Triamine-bearing activated rice husk ash as an advanced functional material for nitrate removal from aqueous solution. *Water Sci Technol.* 2018;79(5):850-6.
- [16] Ayawei N, Ebelegi AN, Wankasi D. Modelling and interpretation of adsorption isotherms. *J Chem.* 2017;2017:1-11.
- [17] Kumar PS, Ramalingam S, Kirupha SD, Murugesan A, Vidhyadevi T, Sivanesan S. Adsorption behavior of nickel (II) onto cashew nut shell: equilibrium, thermodynamics, kinetics, mechanism and process design. *Chem Eng J.* 2011;167(1):122-31.
- [18] Nguyen TA, Fu CC, Juang R-SJCEJ. Effective removal of sulfur dyes from water by biosorption and subsequent immobilized laccase degradation on crosslinked chitosan beads. *Chem Eng J.* 2016;304:313-24.
- [19] Ibrahim D, El-Hemaly S, Abdel-Kerim F. Study of rice-husk ash silica by infrared spectroscopy. *Thermochim Acta.* 1980;37(3):307-14.
- [20] Rajeswari A, Amalraj A, Pius A. Adsorption studies for the removal of nitrate using chitosan/PEG and chitosan/PVA polymer composites. *J Water Process Eng.* 2016;9:123-34.
- [21] Aswin Kumar I, Viswanathan N. Development and reuse of amine-grafted chitosan hybrid beads in the retention of nitrate and phosphate. *J Chem Eng Data.* 2018;63(1):147-58.
- [22] Milmile SN, Pande JV, Karmakar S, Bansiwala A, Chakrabarti T, Biniwale RB. Equilibrium isotherm and kinetic modeling of the adsorption of nitrates by anion exchange Indion N568 resin. *Desalination.* 2011;276(1):38-44.
- [23] Han R, Zhang J, Han P, Wang Y, Zhao Z, Tang M. Study of equilibrium, kinetic and thermodynamic parameters about methylene blue adsorption onto natural zeolite. *Chem Eng J.* 2009;145(3):496-504.
- [24] Yang Y, Wang G, Wang B, Li Z, Jia X, Zhou Q, et al. Biosorption of acid black 172 and congo red from aqueous solution by nonviable *Penicillium YW 01*: Kinetic study, equilibrium isotherm and artificial neural network modeling. *Bioresour Technol.* 2011;102(2):828-34.
- [25] Chanzu HA, Onyari JM, Shiundu PM. Biosorption of malachite green from aqueous solutions onto polylactide/spent brewery grains films: kinetic and equilibrium studies. *J Polym Environ.* 2012;20(3):665-72.
- [26] Iida T, Amano Y, Machida M, Imazeki F. Effect of surface property of activated carbon on adsorption of nitrate ion. *Chem Pharm Bull.* 2013;61(11):1173-7.
- [27] Aharoni C, Ungarish M. Kinetics of activated chemisorption. Part 2.-theoretical models. *Journal of the Chemical Society, Faraday Transactions 1: Physical Chemistry in Condensed Phases.* 1977;73:456-64.
- [28] Tosun I. Ammonium removal from aqueous solutions by clinoptilolite: determination of isotherm and thermodynamic parameters and comparison of kinetics by the double exponential model and conventional kinetic models. *Int J Environ Res Public Health.* 2012;(3):970-84.
- [29] Helfferich FG. Ion exchange. New York: Courier Corporation; 1995.
- [30] Katal R, Baei MS, Rahmati HT, Esfandian H. Kinetic, isotherm and thermodynamic study of nitrate adsorption from aqueous solution using modified rice husk. *J Ind Eng Chem.* 2012;18(1):295-302.